

SIDE COUPLED ACCELERATING STRUCTURE AUTOMATED MEASUREMENT SYSTEM

Peter Steven Prieto, Jim Crisp, Tom Jurgens and Tim Savord
*Fermi National Accelerator Laboratory**
Batavia, Illinois 60510

Abstract

A computer controlled, network analyzer based measurement system was developed for evaluating the side coupled accelerating structure (SCS), which will replace part of the FermiLab linear accelerator. The SCS will boost the Linac energy from 200 MeV to 400 MeV, contributing to the reduction of beam emittance providing a higher intensity beam. The measured parameters include shunt impedance(Z_s), electric field(\vec{E}_0) the total voltage(V), and transit-time factor(T) of the accelerating structure. Also, the stopband, frequency, and Q value of the $\pi/2$ mode are determined.

The first set of parameters (Z_s , \vec{E}_0 , V, T) are measured using a bead-pull perturbation technique. The automated measuring system was designed around an IBM-AT compatible computer, (AST 286), controlling an Hewlett-Packard (HP8510B) network analyzer and a Galil (DMC-400) motor controller, with the National Instruments GPIB interface card. Programs were developed under TurboC (version 2.0) assembler debugger environment. The dispersion measurements are carried out using a sub-set of the above mentioned instruments.

Introduction

The upgrade to the Linac will bring about an increase in beam kinetic energy from 200 MeV to 400 MeV. This will be accomplished by replacing the last four drift tube tanks in the existing Linac with seven modules of the side-coupled structure design. The seven modules break down into four sections of sixteen accelerating cells and fifteen side coupling cells. The sections are connected through bridge couplers[1]. These structures will operate at 805 Mhz, four times the present operating frequency. An automated system was developed for tuning verification and parameter characterization of the structures.

*Operated by the Universities Research Association, Inc. under contract with the U. S. Department of Energy.

The measurements are divided into two classes, dispersion curve and bead-pull.

Dispersion

The goal of this measurement is to assess the stopband of the $\pi/2$ mode. A chain of N coupled cavities will have N cavity chain modes. The resonance, or mode, occurs at the frequency which provides a total phase shift along the chain of $n\pi$ radians, where n is limited to 0,1,...,N-1. The mode which has $\pi/2$ radians of phase shift per cavity, or cell, is chosen because of the coupling efficiency of the bi-periodic structure to the beam and its unique field stability with variations of beam loading and manufacturing inaccuracies.

A sufficient model for analyzing the SCS assumes all accelerating cells and coupling cells are identical. The dispersion relation relates the N mode frequencies with the phase shift per cell. Using ω_1 as the resonant frequency of the accelerating cells, ω_2 that of the coupling cells, κ_1 the coupling coefficient between accelerating and coupling cells, κ_2 that between accelerating cells, and κ_3 that between coupling cells. The dispersion relation can be written as shown below [5].

$$\kappa_1^2 \cos^2 \varphi = \left(1 - \frac{\omega_1^2}{\omega^2} + \kappa_2 \cos 2\varphi\right) \left(1 - \frac{\omega_2^2}{\omega^2} + \kappa_3 \cos 2\varphi\right) \quad (1)$$

In the above equation ω represents each of the N mode frequencies and φ the phase shift per cell. The dispersion equation has two solutions at $\varphi = \pi/2$, $\omega = \frac{\omega_1}{\sqrt{1-\kappa_2}}$, and $\omega = \frac{\omega_2}{\sqrt{1-\kappa_3}}$. The difference in frequency between these two solutions is called the stopband. A sufficiently small stopband insures field and phase uniformity along the SCS. In order to determine the stopband, the frequencies of the 31 modes are measured, then the ω , φ pairs are fit to the dispersion equation(1) using the least squares method[4]. Figure 1 is an example with a typical stopband of

21KHz. Measurements are performed using full cell terminations which provide a phase shift of $N\pi\frac{n+1}{N+1}$ where $n=0,1,...,N-1$.

Bead-Pull Perturbation Technique

The goal of the perturbation measurement is to characterize the field distribution along the beam axis of a module. The phase shift caused by the bead is measured and the fractional detuning computed (eq.2). Then the square of the Electric field per total energy(U) along the beam axis is obtained from the fractional detuning and bead volume (eq. 3).

$$\frac{\partial\omega}{\omega_0} = \frac{\tan \Delta\varphi}{2Q} \quad (2)$$

$$\frac{\vec{E}_0^2}{U} = -\frac{\partial\omega/\omega_0}{3\omega_0\epsilon_0 Vol_{bead}} \quad (3)$$

From this, the voltage across the complete structure can be calculated.

$$\frac{V}{\sqrt{U}} = -\int_0^L \vec{E}_0 \cdot \partial z \quad (4)$$

Finally, the shunt impedance per unit length per total energy is computed,

$$\frac{Z_s}{UL} = \frac{V^2 Q}{\omega_0} \quad (5)$$

where L is the length of the tank in meters.

Hardware

The automated measuring system was designed around an IBM-AT compatible computer, (AST 286), controlling an Hewlett-Packard (HP8510B) network analyzer and a Galil (DMC-400) motor controller with the National Instruments GPIB interface card. For both dispersion and bead-pull measurements the transmission coefficient (S_{21}) is measured between magnetic field probes placed in the terminating cells of the cavity chain. The signal picked up from the cavity is amplified by 22dB to improve the measurement accuracy.

For the bead-pull, a mechanical gantry was made which attaches to the end of the cavity support cradle. Positioning arms can control the bead position along the beam axis with an accuracy of one-one thousandths of an inch. A kevlar thread, holding a brass bead, is run through and over the structure. The bead diameter used for the test is 0.166 inches and is pulled with a DC motor controlled from the AST 286 through a GALIL motor controller (DMC 400). The bead position is provided by a quadrature

shaft encoder, 4000 pulses per revolution, mounted on the DC motor. Limit switches are mounted on the positioning arms to provide home reference and travel limits.

Software

The software was developed with the TurboC compiler, version 2.0. Both dispersion and bead-pull tasks were developed in two separate modules with a third module holding functions common to both. Two complete, stand-alone applications were created. The common module supports functions such as an input data parser, Q value function, 3dB point measurement function, network analyzer parameter update function, GPIB communication functions and system error functions. All major variables and parameters are organized under appropriate structures in the common module and the task-specific applications.

For the dispersion curve measurement, the operator identifies the center frequency of each mode by placing the marker on the peak and then pressing enter. Once all peaks are identified, the system optimizes the frequency and amplitude scale to accurately obtain the frequency and Q of each mode. With these measurements, accelerating cell and side coupled cell frequencies (ω_1, ω_2), coupling coefficients ($\kappa_1, \kappa_2, \kappa_3$), and $\pi/2$ stopband are determined using a least squares fit to the dispersion curve. The results are corrected for temperature, humidity and pressure to predict the behavior of the structure with vacuum.

The bead-pull bases its results on two measured values, phase and bead position. The speed profile of the bead is dependent on the number of sections being measured and the step resolution chosen. After the set-up parameters are entered, the Q value is measured and the structure is driven at the $\pi/2$ frequency of 805 MHz. During the pull, the system reads the phase shift from the analyzer and the bead position from the shaft encoder. Once the bead is out of the structure, $\partial\omega/\omega_0$, $\frac{V}{\sqrt{U}}$, E_0^2 and Z_s are computed. The raw data and the results are displayed using EXCEL version 3.0, a commercially available spread sheet.

Discussion

The hardware is completely in place and tested, except for automated reading of temperature, humidity and pressure. The software has been tested on Section 3, of Module 1, of the SC Linac upgrade. Data validation has been done against manual measurements and results are within 10 KHz for stopband measurement.

The results obtained during a bead-pull follow closely with those obtained from other analyzers and

shunt impedance values correspond to those predicted with Superfish. The value computed for section 3 is 35 M Ω /m compared with 38 M Ω /m based on Superfish (derated by 15 percent).

The software was not designed to account for mis-identified peaks or baseline drifts due to temperature changes during the measurement. A second version of the software could incorporate error-correcting algorithms. Further tests must be carried out with a full module to evaluate the performance of the system.

References

1. R. Noble. "The FermiLab Linac Upgrade," Linac Conference (1990), These Proceedings.
2. P.M. Lapostolle, A.L. Septier. "Linear Accelerators," North Holland Publishing Company, (1970).
3. G.R. Swain. "Lampf 805-MHz Accelerator Structure Tuning and its Relation to Fabrication and Installation," Informal Report LA-7915-MS, (July 1979).
4. P.R. Bevington. "Data Reduction and Error Analysis for the Physical Sciences," McGraw-Hill N.Y.,(1980).
5. E.A. Knapp, B.C. Knapp, and J.M. Potter. "Standing Wave High Energy Linear Accelerator Structures," The Review Of Scientific Instruments. Vol.39, No.7. (July 1968).

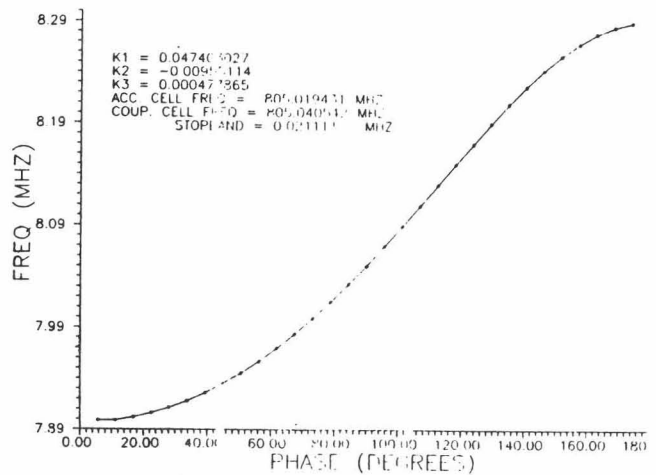


Figure 1: Dispersion curve of section 3. This shows the distribution of the modes about the $\pi/2$ mode, values for the κ 's, stopband and corrected fundamental frequency for accelerating cell and side coupled cell.

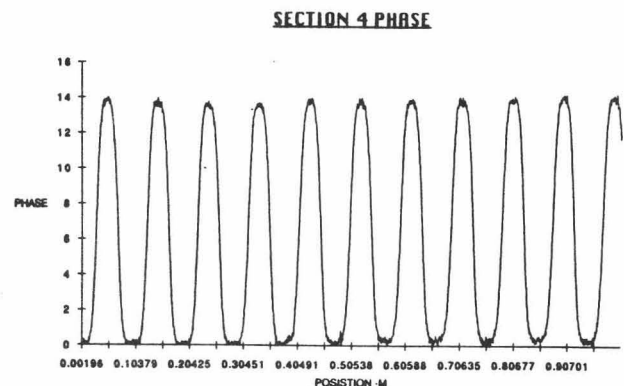


Figure 2: Phase shift produced with a 0.217inch diameter bead, sampled in 2.50 mm step increments